INVESTIGATION ON THE INTERACTIONS BETWEEN ALUMINA-CHROME REFRACTORIES AND ZNO-CONTAINING FAYALITE SLAGS

L. Chen, M. Guo, B. Blanpain, A. Malfliet

KU Leuven, Department of Materials Engineering, Kasteelpark Arenberg 44, BE-3001 Leuven, Belgium

ABSTRACT

In secondary copper smelting processes, ZnO can be present in the fayalitic slag (Fe_xO-SiO_2-based) and thus changes both the physical and chemical properties of the slag. The corrosion behavior of refractory lining by the ZnO-containing secondary copper smelting slag will be consequently affected. Therefore, the interaction between alumina-chrome refractories and ZnO-containing fayalite slags was investigated in this work by static refractory finger tests and alumina crucible tests at 1200 °C under Ar atmosphere. The microstructure of the corroded refractory samples and the slag composition were analyzed by electron probe micro-analysis equipped with wavelength dispersive spectroscopy (EPMA-WDS). The influence of the ZnO level on the Al_2O_3 dissolution and the Al_2O_3/slag interfacial reactions was studied. The experimental results from the alumina crucible tests were interpreted with thermodynamic calculations.

INTRODUCTION

Alumina-chrome (Al_2O_3-Cr_2O_3) refractories are commonly characterized by a high corrosion resistance to acidic slags. Therefore, the corrosion behavior of alumina-chrome refractories in fayalite-based slags has been compared with that of magnesia-chromite refractories [1,2]. The results indicate that alumina-chrome bricks exhibit a better slag corrosion resistance than magnesia-chromite refractories. It is, therefore, expected that the alumina-chrome refractories can also exhibit a superior corrosion resistance to secondary copper smelting slags, thereby extending the lifetime of secondary copper smelters.

Secondary copper smelting is gaining importance in the world copper smelting production [3]. Compared to the primary copper smelting process, new operating conditions and secondary materials with a higher variation in copper content and a higher degree of contamination, are introduced in secondary copper production processes, leading to changes in the composition of the slag, metal or gas phases. The difference in feed results in difference in slag composition. ZnO, for example, can be present in the smelting slag, forming a ZnO-containing fayalite slag [4,5]. Depending on the operation conditions and input materials (for instance, the use of high Zn/ZnO secondaries), the ZnO level in the secondary copper smelting slag can vary [5]. As ZnO is a basic oxide, the addition of ZnO increases the basicity of the slag and decreases the slag viscosity by providing free O^{2-} to break the silica network [6]. Hence, the knowledge about the degradation mechanisms of alumina-chrome refractories in contact with primary copper smelting slags cannot directly be applied to secondary copper smelting processes. As this knowledge is lacking for ZnO-containing fayalite slags, the corrosion behavior of an alumina-chrome refractory in a fayalite slag with ~9 wt.% ZnO was investigated through a refractory finger test at 1200 °C. The effect of the ZnO level in the fayalite slag on the slag/alumina interactions was studied via crucible tests. The impact on the Al_2O_3 dissolution behavior and the refractory/slag interfacial reactions was determined by microstructural and chemical analyses using electron probe micro analysis (EPMA) and scanning electron microscopy (SEM).

EXPERIMENTAL

Materials

ZnO-containing fayalite slags

The composition of the ZnO-containing fayalite (ZFS) slag as supplied by a copper producer is listed in Tab. 1. Other minor elements, such as K, S, P, Mn, and Ni, are accounted as "others". Synthetic fayalite slags were prepared by heat-treating mixed powders of iron, hematite and silica in an iron crucible at 1150 °C for 12 h under Ar atmosphere. ZnO-containing fayalite slags were prepared by mixing different ZnO and CaO contents with the synthetic fayalite slags. The chemical composition of the as-prepared slags is listed in Tab. 2.

Refractory finger and alumina crucible

The cylindrical refractory samples (diameter = ~15 mm; length = ~50 mm) were cut from a commercially available alumina-chrome brick. The chemical composition and physical properties of the investigated alumina-chrome brick are provided in Tab. 3.

Commercially available alumina crucibles (inside diameter = 17.0 mm; height = 30.0 mm, supplied by Avto-G, Slovenia) made with C795 Al_2O_3 (according to DIN EN 60672-3 standard) were used in this work. The alumina crucible consisted of > 95.0 wt% Al_2O_3, ~1.0 wt% CaO, ~1.0 wt% SiO_2 and a small amount of MgO impurities, as measured by EPMA-WDS.

Tab. 1: The chemical composition of the industrial fayalite slag before and after refractory finger tests, as determined by XRF (in wt%)

Slag	Al_2O_3	ZnO	FeO	SiO_2	Na_2O	MgO	CaO	Cr_2O_3	MnO	CuO	MoO_3	PbO	Others
Before	3.1	9.4	55.6	23.7	2.3	0.6	0.7	0.8	0.3	0.6	0.1	1.0	1.8
After	4.4	6.6	58.7	24.1	2.2	0.4	0.8	0.2	0.4	0.2	0	0.6	1.4

Tab. 2. The chemical composition of the synthetic fayalite slags before and after crucible tests, as measured by EPMA-WDS (in wt%)

Exp. no.		ZnO	FeO	SiO_2	Al_2O_3	CaO
Before	S00	0.0	53.6	38.3	6.9	1.1
	S10	10.0	48.3	34.5	6.2	1.0
	S20	20.0	42.9	30.7	5.5	0.9
After	S00	0.0	45.4 ± 0.4	36.6 ± 0.1	9.7 ± 0.4	1.3 ± 0.1
	S10	9.3 ± 0.2	47.1± 0.4	30.4 ± 0.4	5.3 ± 0.1	1.5 ± 0.1
	S20	12.3 ± 0.2	46.6 ± 0.5	28.8 ± 1.4	4.2 ± 0.5	1.4 ± 0.1

Tab. 3: The chemical composition and physical properties of the as-delivered alumina-chrome refractory

Overall composition (in wt%)					Bulk density (g·cm⁻³)	Apparent porosity (%)	Cold crushing strength (MPa)
Al_2O_3	Cr_2O_3	MgO	SiO_2	Fe_2O_3			
82.76	11.00	0.74	0.77	0.09	3.52	12.40	193.72

Experimental set-up and procedure

Static finger tests were performed in a vertical tube furnace (GERO HTRV 100-250/18, with $MoSi_2$ heating elements). The experimental set-up and the procedure has been reported in a previous work [4]. Around 170 g of the industrial ZnO-containing fayalite (ZFS) slag was filled in a Mo crucible (inside diameter = 40 mm; height = 80 mm) and melted at 1200 °C for 1 h. A cylindrical refractory specimen was fixed on a stainless steel bar (φ = 5 mm), preheated for 10 min at a distance of 10 mm above the Mo crucible and then immersed into the melted ZFS slag. After immersion for 4 h, the refractory sample was immediately withdrawn from the furnace and quenched under N_2 gas stream. For the crucible test, approximately 4 g of the as-prepared ZFS slag was filled in the alumina crucible. All three alumina crucibles were put in a larger protective crucible, heated in the vertical tube furnace to 1200 °C, and kept at that temperature for 4 h. After soaking, the protective crucible with its content was removed by a stainless steel rod with a hook from the furnace and quenched under N_2 gas stream. In both the refractory finger and alumina crucible tests, purified Ar gas was blown into the furnace at a flowrate of 0.4 L/min to simulate the reducing atmosphere.

Sample analysis techniques

The worn cylindrical refractory samples were sliced with a diamond saw 10 mm below the slag line, and the quenched crucibles with their contents were cut along the vertical direction. Then, the refractory and crucible specimens were embedded in a low viscosity resin (Epofix) by vacuum impregnation. The embedded specimens were ground with SiC grinding paper, polished with diamond paste and coated with a conductive carbon layer for compositional and microstructural characterization. Compositional analyses were performed with a fully quantitative procedure using electron probe microanalysis coupled with wavelength dispersive spectroscopy (EPMA-WDS, JEOL JXA-8530F). Microstructure images were obtained with a high resolution scanning electron microscope (SEM, Philips XL-30 FEG). The ground slags before and after the finger tests were analyzed with a wavelength-dispersive X-ray fluorescence spectrometer (WD-XRF, Panalytical Zetium) for semi-quantitative analysis. All Fe in this work was calculated in the form of FeO for the purpose of presentation.

RESULTS AND DISCUSSION

Macroscopical observations

Fig. 1 shows the appearance of the as-delivered alumina-chrome refractory finger and the refractory finger sample after testing for 4 h at 1200 °C. Large alumina grains in light gray with a grain size of less than 500 mm can be seen on the surface of the sample before the finger test. The refractory matrix consisting of chrome and smaller alumina grains appears dark gray on the surface of the refractory. After the refractory finger test, a dark, frozen slag layer was observed on the surface of the sample.

Compositional analysis of the slag

Tab. 1 illustrates the changes of slag composition before and after the refractory finger test. The Al_2O_3 concentration in the slag increases from 3.1 wt% before testing to 4.4 wt% after testing, suggesting the dissolution of Al_2O_3 from the alumina-chrome refractory into the ZnO-containing fayalite (ZFS) slag. The high Al_2O_3 solubility limit of 7.9 wt% in the ZFS slag, predicted by FactSage, is the driving force for the dissolution of Al_2O_3. In contrast, the Cr_2O_3 content in the slag remains in a low level of less than 1 wt%, indicating that likewise MgO-chromite refractories [4,5], chrome in alumina-chrome refractories is little attacked by the slag. These results demonstrate that Al_2O_3 in alumina-chrome refractories is predominantly corroded by the ZFS slag, whereas the chrome is little attacked.

The changes in slag composition after the alumina crucible tests are shown in Tab. 2. The Al_2O_3 content in the slag increased from

6.9 wt% to 9.7 wt% in Test S00, but slightly decreased from 6.2 wt% to 5.3 wt% in Test S10 and 5.5 wt% to 4.2 wt% in Test S20. A similar trend is observed for the Al_2O_3 solubility, as shown in Fig. 2, predicted by thermodynamic calculations using FactSage as this is for S00, S10 and S20 respectively 13.6, 10.6 and 7.6 wt%. This indicates that the driving force for the Al_2O_3 dissolution in the ZFS slag decreases with the increase of ZnO content in the fayalite slag having the same FeO/SiO_2 ratio.
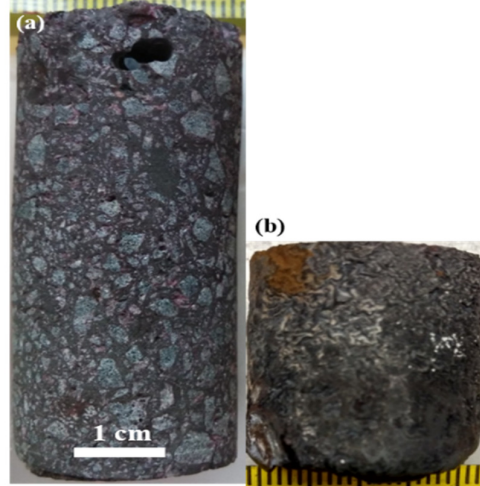

Fig. 1: Pictures of the Al_2O_3-chromite refractory sample (a) before and (b) after refractory finger test.
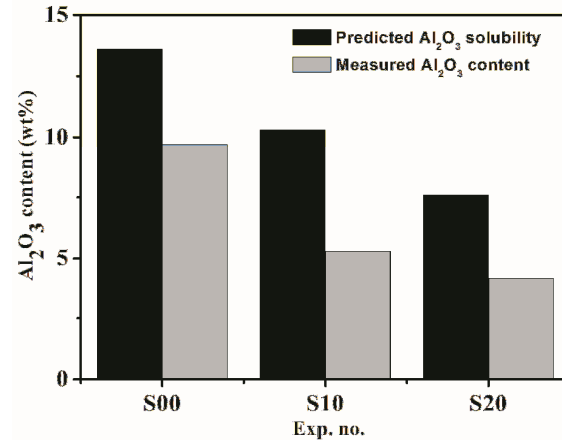

Fig. 2: Comparisons of the predicted Al_2O_3 solubility and measured Al_2O_3 content in the tested slag from crucible tests.

Microstructural analyses

The worn microstructures of the tested refractory finger sample are shown in Fig. 3. The surface of the sample is covered with a frozen slag layer with a thickness of ~240 μm (Fig. 3a). A concave outline is observed on the surface of alumina grains, due to the corrosion of alumina by the slag. In comparison, the chrome-containing refractory matrix is less attacked by the slag. These observations further confirm that alumina in the refractories is predominantly corroded by the ZFS slag. The slag infiltrated into the grain boundary and open pore network with a depth of around 2 mm. Large cracks can be seen between the alumina grains and the refractory matrix, which might be generated during quenching or cutting of the worn refractory sample. A dense, continuous $(Fe_x,Zn_{1-x})Al_2O_4$ spinel layer is observed at the alumina grain/slag interface (Fig. 3b). The presence of ZnO in the spinel suggests that this phase is freshly formed upon the dissolution of the alumina grains at their interface with the slag. It is believed that this $(Fe_x,Zn_{1-x})Al_2O_4$ spinel formed at the slag/alumina interface once the slag was locally saturated with Al_2O_3.

The observations from the refractory finger tests could be summarized as follows: (1) similar to the MgO-chromite

refractories [4,5], alumina in the alumina-chrome refractories is predominantly attacked by the ZFS slag, whilst the chromite reacts less with the slag; (2) the corrosion of alumina is mainly caused by the dissolution of Al_2O_3 into the slag, the high solubility limit of Al_2O_3 in the slag is the driving force for the Al_2O_3 dissolution; (3) $(Fe_x,Zn_{1-x})Al_2O_4$ spinel is precipitated at the slag/alumina interface once the slag is locally saturated with Al_2O_3; (4) the ZFS slag penetrates into the refractory with a depth of around 2 mm after 4 h interaction, through the open pore network and grain boundaries.
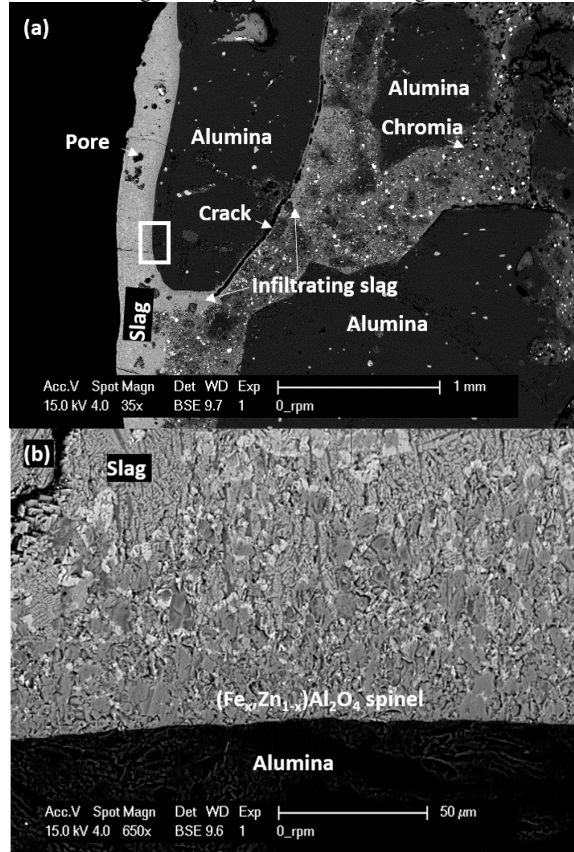

Fig. 3: BSE images of (a) the alumina-chromite refractory/slag interface and (b) the enlarged view of the selected area in (a), from the refractory finger test, showing the slag infiltration and refractory/slag interactions.

Fig. 4 shows the microstructures at the interface between the alumina crucible and ZFS slags with various ZnO levels. $(Fe_x,Zn_{1-x})Al_2O_4$ spinel ($FeAl_2O_4$ spinel for Test S00) precipitated at the crucible/slag interface, forming a continuous layer. $(Fe_x,Zn_{1-x})Al_2O_4$ spinel grains were also observed in the slag close to the alumina crucible, whereas they were not found in the bulk slag. It can be also seen that the grain size of the $(Fe_x,Zn_{1-x})Al_2O_4$ particles gradually decreases with the increase of the distance from the crucible. These observations further confirm that $(Fe_x,Zn_{1-x})Al_2O_4$ spinel generated at the slag/alumina interface once the slag is locally saturated with Al_2O_3. As shown in Fig. 4 that a dense $(Fe_x,Zn_{1-x})Al_2O_4$ spinel layer is observed in Test S10 and S20, whereas slag can be found in the $FeAl_2O_4$ spinel layer in Test S00. These observations suggest that Al_2O_3 dissolved into the slag directly in Test S00, but indirectly in Test S10 and S20. These results indicate that the solubility limit was reduced and Al_2O_3 dissolved into the ZFS slag indirectly, and consequently the dissolution rate of Al_2O_3 would be lowered in the high ZnO level slag.
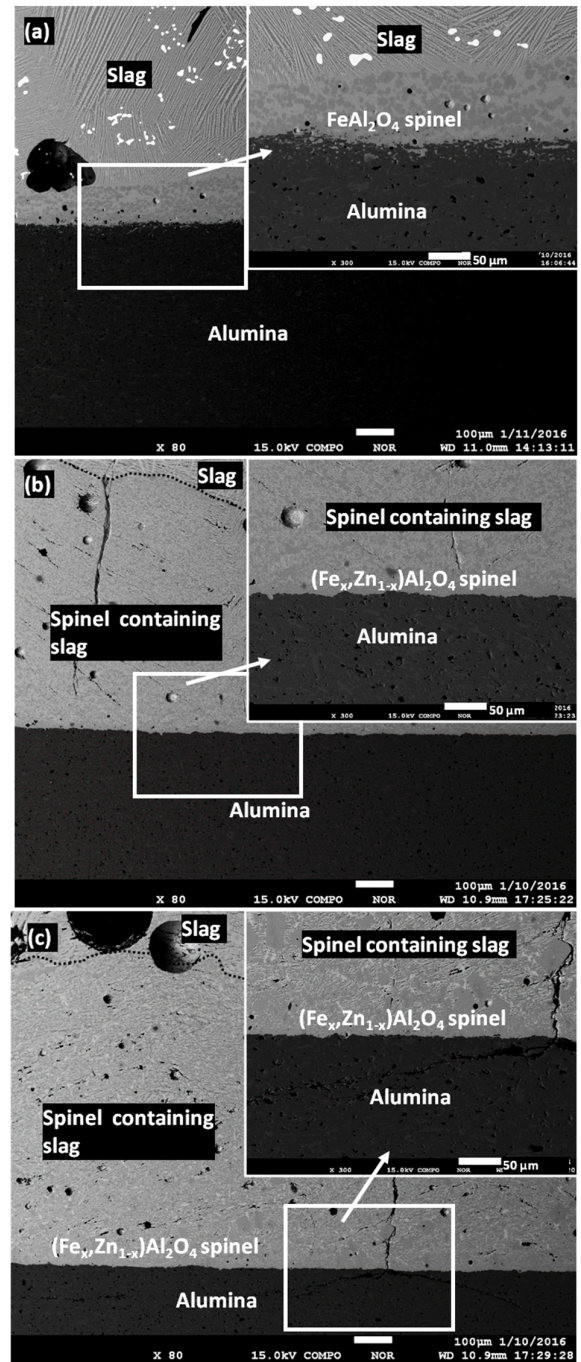

Fig. 4: BSE images of the crucible/slag interface from the alumina crucible tests (a) S00, (b) S10 and (c) S20. The insert images are detailed micrographs at the interfaces of the selected zones, showing the influence of ZnO levels on the slag/alumina interactions.

CONCLUSIONS

The interactions between alumina-chrome refractory and ZnO-containing fayalite (ZFS) slags were investigated. This was performed by static refractory finger tests in industrial fayalite slag with ~9 wt% ZnO and alumina crucible tests containing synthetic fayalite slags with ZnO contents from 0 to 20 wt% at 1200°C for 4 h under protective atmosphere. Based on the microstructure observations and chemical composition analyses, the conclusions can be drawn:

(1) Alumina in alumina-chrome refractories was predominantly corroded by the ZFS slag, due to the dissolution of Al_2O_3 into

the slag. In comparison, chrome in the refractory was little corroded by the slag. With the increase of ZnO content in the slag, the Al_2O_3 dissolution was hindered.

(2) The ZFS slag infiltrated into alumina-chrome refractories through open-pore network and grain boundaries in a depth of 2 mm after 4 h interaction.

(3) $(Fe_x,Zn_{1-x})Al_2O_4$ spinel precipitated from the slag once the slag is locally saturated with Al_2O_3. $(Fe_x,Zn_{1-x})Al_2O_4$ spinel can form a dense layer at the slag/alumina interface, changing the Al_2O_3 dissolution from a direct way to an indirect one. As a result, the dissolution rate of Al_2O_3 into ZFS slags would be lowered.

REFERENCES

[1] Rigby A.J. The use of alumina-chrome refractories in the high wear areas of anode refining vessels. In: Proceeding of Copper, Santiago, Chile, 2013 pp.497-505.

[2] Zou L, Jiang M, Qian Y, Shi X, Simulation study on corrosion resistance of Al_2O_3-Cr_2O_3 and MgO-Cr_2O_3 bricks to ISA furnace slag. Refractories/Naihuo Cailiao (in Chinese) 2007, **41**(3): 180-182.

[3] International Copper Study Group. The world copper Factbook 2013, Lisbon, Portugal; 2013.

[4] Chen L, Guo M, Shi H, Huang S, Jones PT, Blanpain B, Malfliet A. Effect of ZnO level in fayalite slags on slag/magnesia–chromite refractory interactions. J Eur Ceram Soc. 2016 Jul; 36(7): 1821–8.

[5] Chen L, Guo M, Shi H, Scheunis L, Jones PT, Blanpain B, Malfliet A. The influence of ZnO in fayalite slag on the degradation of magnesia-chromite refractories during secondary Cu smelting. J Eur Ceram Soc. 2015 Sep; 35(9): 2641–50.

[6] Sumita S, Takano H, Morinaga K, Yanagase T. Viscosity and electrical-conductivity of Na_2O–SiO_2–ZnO and CaO–SiO_2–ZnO Melts. J Jpn Inst Met. 1982; 46 (3): 280–5.